Robust Beam-Pointing and Attitude Control of a Flexible Spacecraft

Joseph S-C. Yuan*
Spar Aerospace Limited, Toronto, Canada
and
Michael E. Stieber†
Department of Communications, Ottawa, Canada

This paper studies the problem of simultaneously controlling the communications beams and the attitude angles of the main bus of a flexible spacecraft. The controller is a multivariable proportional-integral compensator augmented by a Kalman filter. Two design methods have been explored: the first method is based on eigenvalue analysis, while the second makes use of singular value criteria. Both approaches result in a controller that is robust in the presence of the residual modes omitted from the design model. The singular value method, however, is shown to be far more conservative than the eigenvalue method.

Introduction

IN order to minimize the ground segment costs and maximize the utilization of the frequency spectrum, the next generation of communications satellites will need to be configured to provide narrow communications beams with very accurate pointing. Typically, this implies the use of large-antenna reflector/feed systems to generate beam patterns small enough to allow the use of modestly sized (therefore low-cost) ground receivers. Furthermore, for multiareas coverage, many such reflectors may be needed on a single spacecraft.

As a result, this class of so-called third-generation spacecraft are generally characterized by large distributed masses connected by deployable, lightweight beam structures. Also, depending on the selection of the relative locations of the reflectors and their feeds, the configurations of the spacecraft are not necessarily symmetrical as in conventional satellites.

A typical example of third-generation spacecraft is the operational mobile communications satellite (MSAT) shown in Fig. 1, which is under consideration by the Department of Communications in Canada. The spacecraft is composed of a 44-m-diam reflector supported at its hub by an L-shaped (24- × 47-m) tower structure connected to the main bus. The latter also carries a rectangular (4- × 38-m) solar array delivering 8.2 kW of power. The total mass of the spacecraft is about 3500 kg; however, its c.m. resides outside the physical structure. With a beamwidth of 0.5 deg, a pointing accuracy of .05 deg about the line-of-sight is required. Apart from the main bus, none of its appendages could be assumed to be rigid.

Due to offsets between the centers of mass and pressure, the nonsymmetrical configuration results in environmental (mainly solar and gravity gradient) torques significantly larger than those experienced in earlier satellites. Furthermore, the placement of the actuators (Fig. 2) is far from optimal from the dynamic standpoint. Any slight misalignment or mismatch of the thrusters could cause significant disturbances during stationkeep and momentum dump maneuvers.

Received June 4, 1985; presented as Paper 85-1967 at the AIAA Guidance, Navigation and Control Conference, Snowmass, CO, Aug. 19-21, 1985; revision received Oct. 4, 1985.

*Staff Engineer, Remote Manipulator Systems Division. Member AIAA.

†Engineer, Spacecraft Control Systems, Communications Research Centre.

The main control problem is to maintain the pointing stability of the communications beam as well as the attitude of the main bus despite nontrivial structural flexibility and disturbances arising from the nonsymmetrical configuration of the spacecraft.

The dynamic model of a structurally flexible system necessarily includes a large number of modes, only a limited number of which could be accommodated in the controller design. Hence, the control system must also be designed to be robust in the presence of the unmodeled dynamics (i.e., no adverse "spillover" effects).

The control problems for this spacecraft have been the subject of a number of studies conducted over the last few years.[1-3] Due to the structural flexibility of the tower connecting the reflector to its feeds, the conventional approach of controlling the beam by stabilizing the attitude of the main bus is no longer adequate. Also, the intuitive approach of augmenting the bus attitude control system with a separate antenna pointing mechanism is not feasible due to the dynamic coupling between these control loops caused by noncolocated sensing and actuation. Hence, a multivariable control philosophy must be adopted such that the beam angles and the attitude of the main bus can be controlled simultaneously. This paper investigates how such a control system can be designed to be robust in the presence of dynamic spillover.

Model Description

Evaluation Model

The dynamic models for the flexible elements (solar array, tower, and reflector) of the spacecraft have been developed elsewhere[4] and will not be detailed here. In essence, the initial model consists of 14 physical coordinates and 94 structural coordinates distributed as follows:

1) *Physical coordinates*: These consist of 6 coordinates for the absolute translation and rotation of the main bus, 2 degrees of freedom for the angular motion of the gimbals located at the hub of the reflector, and 6 coordinates representing the relative displacement and orientation between the tower tip and the main bus.

2) *Structural coordinates*: Initially, these comprised 38 modes for the solar array, 14 for the tower, and 42 for the reflector. After modal momentum and frequency considerations,[4] the numbers of coordinates for the array and the reflector were reduced to 27 and 18, respectively.

The physical and structural coordinates can be converted via a standard modal decomposition into a set of decoupled

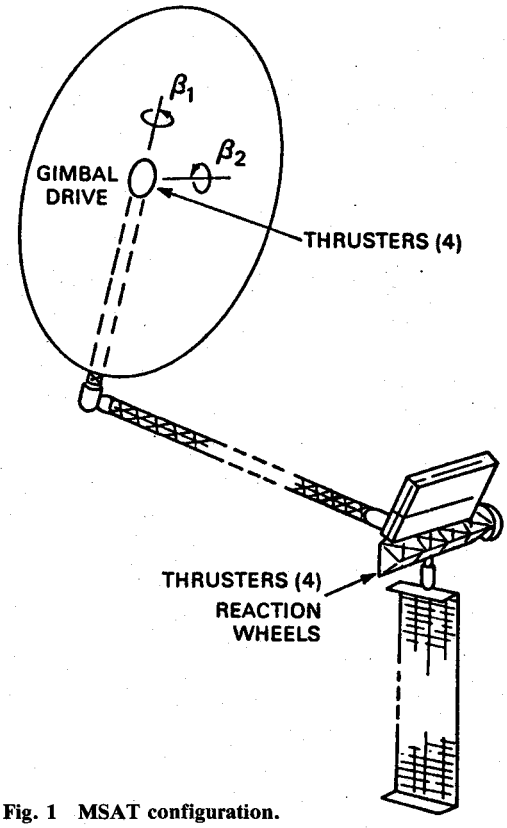

Fig. 1 MSAT configuration.

coordinates representing the natural modes of the entire spacecraft. These are denoted by

$$\phi = [\phi_r^T \phi_e^T]^T \tag{1}$$

where ϕ_r contains 8 rigid-body modes (3 each for rotation and translation and 2 for the communications beam) and ϕ_e contains the remaining 65 elastic modes. Since we were concerned only with attitude and beam control, the 3 translational modes were deleted from the model.

With the aid of modal cost analysis,[5] the number of elastic modes was further reduced to 11. These, togther with the 5 rigid-body modes, were then adopted as the evaluation model for this study and can be written in the state variable form as

$$\dot{x}_p = A_p x_p + B_p u + B_d u_d \tag{2}$$

where

$$x_p = [\phi^T \dot{\phi}^T]^T \epsilon R^{32}, \quad u \epsilon R^7, \quad u_d \epsilon R^{15}$$

Here the control input (u) consists of two gimbal torques and 5 linearly independent forces derived from the 8 thruster forces shown in Fig. 2. A disturbance input (u_d) comprising 15 forces and torques distributed throughout the spacecraft has been included to model the effects of both external (environmental) and internal (momentum dump and stationkeep) disturbances.

It is assumed that all the physical coordinates (less the bus translation), as well as the rates of the bus attitude and gimbal angles, are measurable. Thus, there are a total of 16 measurements which can be written as

$$y = C_p x_p \epsilon R^{16} \tag{3}$$

As stated before, the main objective here is to control the beam angles (elevation and azimuth about the line-of-sight) and the attitude of the main bus. In addition, we shall also

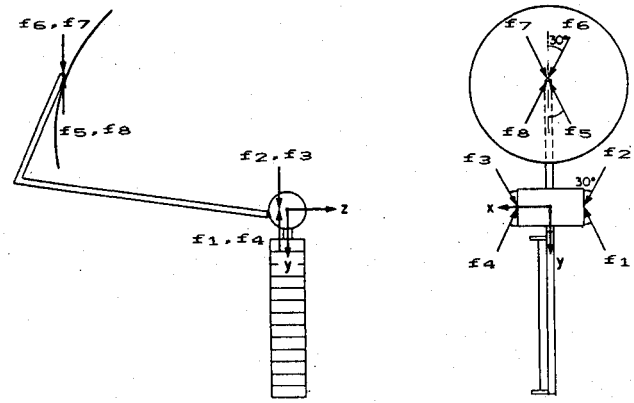

Fig. 2 Thruster location on MSAT.

Table 1 Modal costs of elastic modes in evaluation model

Mode no.	Frequency, rad/s	Modal costs
3	0.239522	0.205407*E* 2
2	0.151178	0.129580*E* 1
1	0.124348	0.487066*E* 0
6	0.779434	0.211837*E* 0
9	1.551440	0.183379*E* 0
11	13.804100	0.154724*E* 0
4	0.556322	0.135429*E* 0
10	10.046000	0.131883*E* 0
5	0.690179	0.657074*E*−2
7	1.022720	0.402586*E*−2
8	1.087340	0.117715*E*−2

allow beam steering by controlling the two gimbal angles. Thus, there are a total of 7 outputs to be controlled; these can be related to the state of the evaluation model as

$$z = D_p x_p \epsilon R^7 \tag{4}$$

In summary, the complete evaluation model (of order 32) consists of 5 rigid and 11 elastic modes, 7 control inputs, 16 measuremnets, 15 disturbances, and 7 outputs to be controlled. Furthermore, it can be shown that with this chosen set of inputs and outputs, the model is completely controllable and observable and has no transmission zeros.

Design Model

For the purpose of control design, an appropriate low-order design model must first be generated from the evaluation model. The modal cost analysis method[5] ranks the elastic modes according to their contributions toward a quadratic cost function of the form

$$\int_0^\infty z^T R_1 z dt \tag{5}$$

where R_1 is a suitably chosen weighting matrix. For this study, we weighted the outputs z in inverse proportion to the square of their maximal allowable tracking errors.

A typical distribution of modal costs is shown in Table 1, which was computed for maximal tracking errors of .03 deg in bus roll and pitch, 0.1 deg in bus yaw (less critcal for North American coverage), .01 deg in beam errors, and .03 deg in the gimbal angle errors. Based on this modal ranking, the 4 elastic modes with the largest modal costs (modes 3, 2, 1, and 6), together with all 5 of the rigid-body modes, were retained to form the control design model, which can be expressed in state

variable form as

$$\dot{x}_c = A_c x_c + B_c u + B_{dc} u_d$$

$$y = C_c x_c, \qquad z = D_c x_c \tag{6}$$

Here x_c is an 18-vector of the modes retained in x_p. The subscript c denotes the truncated version of the corresponding matrices in the evaluation model given by Eqs. (2-4). The system eigenvalues of both the evaluation and design models are listed in Table 2.

Design Requirements

The control problems discussed earlier can now be formulated in terms of the following design requirements based on the design model [Eq. (6)].

1) *Internal stability*: All the internal states in x_c must be stabilized. Note that, in principle, this also damps any vibration caused by the structural modes included in x_c.

2) *Steady-state tracking*: The output z must be made to track a constant reference z_0 with zero steady-state errors.

3) *Disturbance rejection*: The above properties must hold in the presence of any constant disturbance u_d, such as slowly varying environmental torques and forces.

4) *Robustness*: The above properties must still hold when the controller is applied to the evalaution model [Eqs. (2-4)].

Compensator Configuration

A compensator that will meet requirements (1-3) above is given by a standard proportional-integral controller[6] (Fig. 3):

$$\dot{p} = z - z_0 \tag{7a}$$

$$\dot{\hat{x}}_c = A_c \hat{x}_c + B_c u + K_c (y - C_c \hat{x}_c) \tag{7b}$$

$$u = -F_1 \hat{x}_c - F_2 p + u_0 \tag{7c}$$

The integrators in Eq. (7a) compensate for constant disturbances, while Eq. (7b) represents either a Kalman filter or a Luenberger observer. The feedforward bias term (u_0) in the regulator equation (7c) allows the controller to track nonzero setpoints.

In the case of a Kalman filter design, we recast the design model equation (6) in the form

$$\dot{x}_c = A_c x_c + B_c u + B_{dc}(u_d + w_d)$$

$$y = C_c x_c + w_m \tag{8}$$

where w_d and w_m model the random input disturbance and measurement noise, respectively. For the filter design, these may be assumed to be uncorrelated zero-mean white noise processes with intensities given by

$$\begin{bmatrix} w_d \\ w_m \end{bmatrix} \sim \begin{bmatrix} v_1 & 0 \\ 0 & \rho_1 v_2 \end{bmatrix} \tag{9}$$

For any given noise intensities, an optimal estimator is designed by solving for the steady-state solution of an algebraic matrix Riccati equation.[6] The measurement noise intensity is parameterized here by the scalar quantity ρ_1. Note that a large positive value of ρ_1 would indicate considerable uncertainty in the measurement noise so that a filter with relatively slow dynamics would typically result. Conversely, the filter response may be speeded up by reducing the value of ρ_1. In this manner, the scalar quantity ρ_1 may be used to tune the "bandwidth" of the filter. (The classical notation of "bandwidth" is not well defined for multi-input-multi-output systems. The term is used here loosely to characterize the response speed of the dominant modes.)

Table 2 Open-loop system eigenvalues

Real	±Imaginary
Evaluation model	
0.0	0.0
(repeated 10 times)	
−1.17460	13.8041
−0.523904	10.0460
−7.505000E−02	1.55144
−6.063532E−03	1.08734
−8.059164E−03	1.02272
−2.110881E−02	0.779434
−5.531155E−03	0.690179
−8.557398E−03	0.556322
−8.529988E−04	0.151178
−1.704503E−03	0.239522
−9.230091E−04	0.124348
Design model	
0.0	0.0
(repeated 10 times)	
−2.107499E−02	0.779345
−9.230071E−04	0.124347
−1.704499E−03	0.239518
−8.530011E−04	0.151178

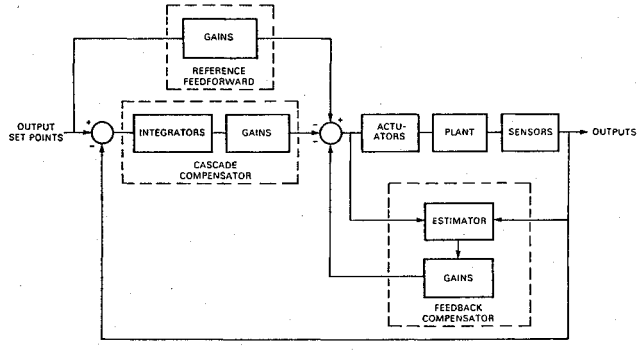

Fig. 3 Control system configuration.

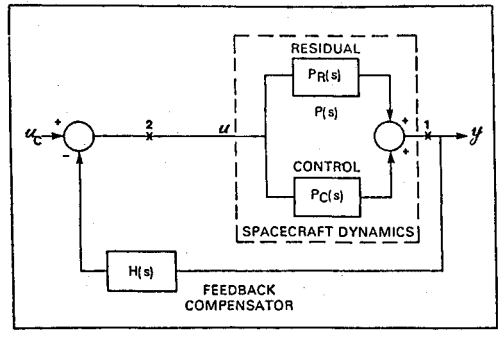

Fig. 4 An alternative representation of a control system for flexible spacecraft.

The gains (F_1, F_2) in the regulator equation (7c) may be determined by minimizing a cost function of the form

$$\int_0^\infty (z'^T R_1 z' + p^T R_1 p + \rho_2 u'^T u') \mathrm{d}t \tag{10}$$

where $z' = z - z_0$ and $u' = u - u_0$. The output weighting matrix R_1 is chosen to be the same as the weighting matrix shown in Eq. (5) for the modal cost analysis. The optimal solution is also obtained by solving for the steady-state solution of a matrix Riccati equation. As before, the scalar ρ_2 is introduced here to tune the bandwidth of the regulator.

Table 3 Typical stability pattern generated by eigenvalue method

		Filter designs (log ρ_1)								
		1	2	3	4	5	6	7	8	9
Regulator designs (log ρ_2)	1	*	*	*	*	*	*	*	*	*
	2	*	*	*	*	0	0	*	*	*
	3	*	*	*	*	0[a]	*	0	*	*
	4	*	*	*	0	0	0	0	0	0
	5	*	*	0	0	0	0	0	0[b]	0
	6	0	0	0	0	0	0	0	0	0
	7	0	0	0	0	0	0	0	0	0
	8	0	0	0	0	0	0	0	0	0[c]
	9	0	0	0	0	0	0	0	0	0

N.B.: * = unstable; 0 = stable.
[a]Nominal controller (a). [b]Nominal controller (b). [c]Nominal controller (c).

Design Results

It is known[6] that the properties of steady-state tracking and disturbance rejection are guaranteed, provided the closed-loop system is asymptotically stable. Furthermore, if the closed-loop system remains stable when the compensator is applied to the evaluation model, we will have demonstrated robustness of the controller design to the residual dynamics.

Two methods of searching for such a robust compensator have been investigated. The first, and the most straightforward, approach simply examines the closed-loop eigenvalues of the evaluation model. In the second approach, robustness is built directly into the design through the use of singular value criteria.

Eigenvalue Method

This method separately computes the optimal filter equation (7b) and regulator equation (7c) over a range of values for ρ_1 and ρ_2. The closed-loop eigenvalues of the evaluation model are then examined for stability. A typical stability pattern that results is shown in Table 3; this would then allow the designer to select the "best" combination of filter and regulator to form the compensator.

The closed-loop system eigenvalues for three nominal controllers a, b, and c are listed in Tables 4-6, which indicate the closed-loop system indeed to be asymptotically stable. Furthermore, by comparing the dominant eigenvalues of the three controller ane may conclude that controller a has a larger bandwidth than controller b, whose bandwidth, in turn, exceeds that of controller c.

To demonstate robustness with regard to variations in the design parameters, the gains in controller a were modified by first multiplying all the gains in the estimator by a constant factor representing deviations of 1-20% from their nominal values. The gains of the regulator were then each truncated to various numbers of significant figures representing round-off errors. Table 7 lists the number of unstable closed-loop eigenvalues that resulted when the modified controller was again applied to the evaluation model. It is clear that the system's stability is highly insensitive to variations in the numerical accuracy of the regulator gains.

Singular Value Method

The eigenvalue method described above suffers from a major drawback: robustness is assured only for the specific evaluation model used in the eigenvalue analysis, and no conclusion can be drawn regarding the possible destabilizing effects of parametric perturbation in the model.

In recent years, a generalization of the classical Nyquist criterion has been used to derive sufficient conditions of robustness for multi-input-multi-output systems.[7-9] One of the first of many attempts to apply this approach to flexible spacecraft is reported in Ref. 10.

Table 4 Closed-loop evaluation system eigenvalues with controller a

Real	± Imaginary
−1.88526	20.8036
−0.106470	11.0589
−4.749030E−02	1.50120
−0.948199	0.00000
−6.772254E−03	1.09315
−2.407224E−02	1.03942
−8.720900E−02	0.887757
−0.232469	0.798301
−2.201277E−02	0.779488
−7.746885E−03	0.656300
−0.364507	0.00000
−0.122789	0.231737
−3.498022E−02	0.243471
−0.271089	0.00000
−2.867876E−02	0.233024
−0.150244	0.133151
−0.158051	0.131145
−9.296904E−03	0.157208
−5.771793E−03	0.148253
−1.294118E−02	0.136720
−5.728888E−02	0.140760
−7.193102E−02	0.111687
−0.175142	4.864297E−02
−2.631942E−02	7.777574E−02
−5.640861E−02	6.922522E−02
−1.563456E−03	0.00000
−1.451082E−03	0.00000
−0.135853	0.00000
−7.339645E−02	2.046178E−02
−0.126331	0.00000
−0.103870	0.00000
−0.107568	0.00000
−0.109545	0.00000
−0.106783	0.00000

In short, the technique is based on the properties of the return difference matrix obtained by breaking the loop at some point in the closed-loop system. As an example, consider the system described in Fig. 4, which is an alternative representation of the system shown in Fig. 3, with the feedforward path removed (the latter has no influence on the stability of the closed-loop system). The return difference matrix is given by

$$I+H(s)P(s) \tag{11a}$$

with the loop broken at the input (point 2), but becomes

$$I+P(s)H(s) \tag{11b}$$

when the loop is broken at the output (point 1) of the system.

A straightforward application of the robustness criteria of Refs. 7-9 reveals that a sufficient condition for closed-loop system stability is

$$\underline{\sigma}[H(j\omega)P_R(j\omega)] < \underline{\sigma}(I + H(j\omega)P_C(j\omega)], \quad \omega > 0 \tag{12a}$$

for loop breaking at the input, and

$$\underline{\sigma}(P_R(j\omega)H(j\omega)] < \underline{\sigma}(I + P_C(j\omega)H(j\omega)], \quad \omega > 0 \tag{12b}$$

for loop breaking at the output Here σ and $\underline{\sigma}$ denote the maximum and the minimum singular values, respectively, of a matrix; they are defined as follows:

$$\bar{\sigma}(A) = [\text{max. eigenvalue of } A^*A]^{1/2}$$

$$\underline{\sigma}(A) = [\text{min. eigenvalue of } A^*A]^{1/2}$$

where $(\cdot)^*$ denotes the conjugate transpose of a complex matrix. Thus, the maximum singular value of a matrix is, in fact, a standard (spectral) matrix norm. Note that the conditions in Eq. (12) effectively impose a frequency-dependent upper bound on the magnitude of the residual modal dynamics, regardless of how the latter is structured. Hence, the singular value method has the powerful advantage of guaranteeing robustness for a broad class of perturbation dynamics (with possibly unknown structure).

Unfortunately, as stated above, the criteria are not very useful in the present case since the compensator $H(s)$ contains open integrators (i.e., 1/s terms); the left-hand side of Eq. (12a) or Eq. (12b) approaches infinity at low frequencies, and the bound becomes meaningless.

Using a procedure similar to one described in Ref. 9, it can be shown that a sufficient condition for robustness is given by

$$\bar{\sigma}[W(j\omega)P_R(j\omega)] < 1, \quad \omega > 0 \tag{13a}$$

for input loop breaking, and

$$\bar{\sigma}[P_R(j\omega)W(j\omega)] < 1, \quad \omega > 0 \tag{13b}$$

for output loop breaking. The transfer matrix $W(s)$ is defined in both cases by

$$W(s) = [I + H(s)P_C(s)]^{-1}H(s)$$

$$= H(s)[I + P_C(s)H(s)]^{-1} \tag{14}$$

Note that, due to pole-zero cancellations in $W(s)$, the criteria in Eq. (13) remain bounded at low frequencies. Note also that the conditions of Eq. (12) imply those of Eq. (13), but not conversely, indicating the latter to be weaker (therefore, less conservative) conditions.

Finally, as a corollary, a sufficient condition for both the conditions in Eq. (13) is given by

$$\bar{\sigma}[P_R(j\omega)] < 1/\bar{\sigma}[W(j\omega)], \quad \omega > 0 \tag{15}$$

which provides a direct bound on the magnitude of the residual dynamics.

During the design of the compensator, the above criteria would be applied to various optimal compensators, each characterized as before by the scalar parameters ρ_1 and ρ_2. By "tuning" these parameters, the robustness criteria could be made to be satisfied over the frequency range of interest (i.e., of the control and residual modes).

In principle, any one of the above criteria may be used. In practice, however, the choice is somewhat dependent on the computational resources available to the designer. While the product $[WP_R]$ of Eq. (13a) is a 7×7 transfer matrix, $[P_RW]$ appears as a 16×16 matrix in Eq. (13b). Even though both matrices are of order 57, there is nevertheless a considerable difference in computational requirements between the two criteria.

Table 5 Closed-loop evaluation system eigenvalues with controller b

Real	± Imaginary
−1.19875	13.8977
−0.498075	10.0952
−7.519076E−02	1.55079
−6.057926E−03	1.08736
−7.844543E−03	1.02313
−2.114781E−02	0.779435
−2.308472E−02	0.779235
−5.290799E−03	0.690755
−6.508498E−03	0.559236
−4.603481E−03	0.239577
−1.748159E−02	0.239172
−1.327117E−03	0.151118
−2.580526E−03	0.151261
−3.571205E−03	0.124500
−7.412824E−03	0.124579
−6.114523E−02	0.106077
−0.122245	0.00000
−0.128175	0.00000
−5.547057E−02	9.945473E−02
−3.212011E−02	5.513454E−02
−6.293226E−02	0.00000
−2.987509E−02	4.714444E−02
−5.269355E−02	3.358003E−03
−1.820735E−02	3.447216E−02
−1.561635E−04	1.186506E−06
−1.625141E−02	1.556341E−02
−2.503957E−02	2.358937E−02
−2.134332E−02	2.057110E−02
−2.399166E−02	2.23965E−02
−2.324784E−02	1.939353E−02

Table 6 Closed-loop evaluation system eigenvalues with controller c

Real	± Imaginary
−1.17568	13.8087
−0.522505	10.0484
−7.506467E−02	1.55141
−6.063076E−03	1.08735
−8.041424E−03	1.02274
−2.111997E−02	0.779452
−2.128584E−02	0.779316
−5.508902E−03	0.690211
−8.381309E−03	0.556466
−1.714496E−03	0.239521
−5.758929E−03	0.239484
−8.544516E−04	0.151178
−1.156628E−03	0.151187
−9.408765E−04	0.124348
−2.487296E−03	0.124382
−2.171600E−02	3.761828E−02
−2.109818E−02	3.640780E−02
−4.342708E−02	0.00000
−4.353906E−02	0.00000
−1.129876E−02	1.9531010E−02
−9.992796E−03	1.694624E−02
−2.249523E−02	0.00000
−7.304401E−03	1.329803E−02
−1.380580E−02	1.355861E−02
−1.322168E−02	1.288271E−02
−1.185563E−02	1.172282E−02
−1.237899E−02	1.154182E−02
−9.039112E−03	8.856062E−03
−1.955276E−02	0.00000
−1.569339E−02	0.00000
−6.985760E−06	5.241709E−08

Table 7 Number of unstable closed-loop system eigenvalues due to round-off and parametric errors [controller a]

Change in filter gains, %	No. of significant figures retained in regulator gains				
	Nominal	5	3	2	1
Nominal	0	0	0	0	0
1	0	0	0	0	0
5	0	0	0	0	0
10	2	2	2	2	2
20	4	4	4	4	4

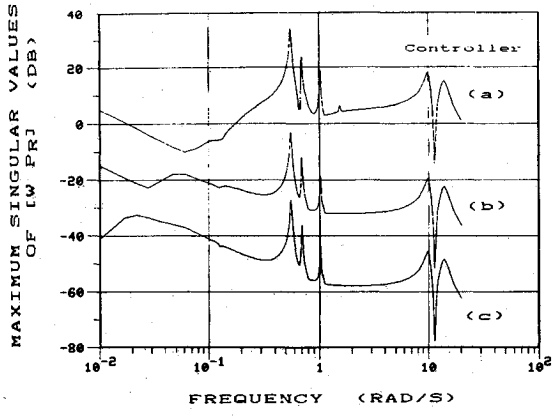

Fig. 5 Singular value plots for condition (13a).

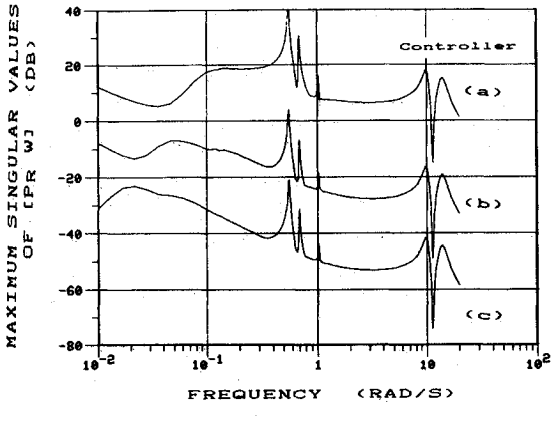

Fig. 6 Singular value plots for condition (13b).

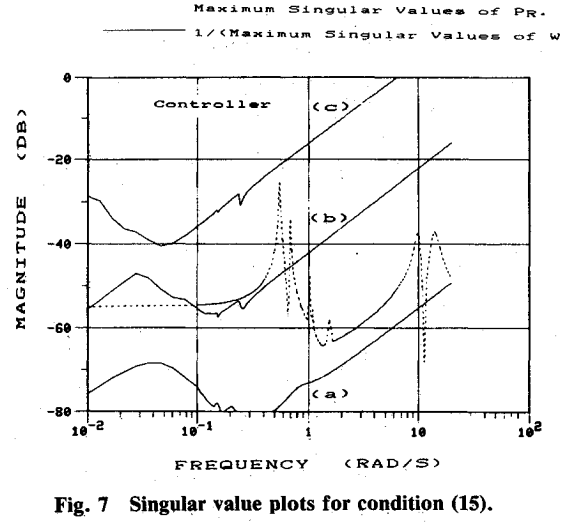

Fig. 7 Singular value plots for condition (15).

The singular value condition of Eq. (13a) is plotted in Fig. 5 for the three compensators identified as controllers a, b, and c in Table 3, all of which have been shown by the eigenvalue method to be stable when applied to the evaluation model. However, it is seen that the criterion is satisfied here only for controllers b and c; no stability conclusion could be drawn on controller a.

Figure 6 shows the robustness criterion of Eq. (13b) plotted for the same three controllers. This time, however, stability is guaranteed only for controller c; the criterion is violated by both controllers a and b.

Finally, the criterion of Eq. (15) is plotted in Fig. 7 for the three controllers. Again, only controller c is shown to be admissible.

Based on bandwidth consideration, it appears that both the conditions in Eq. (13b) and Eq. (15) are more conservative than that of Eq. (13a) because the design that results (controller c) has the smallest bandwidth of the three controllers. Since condition (15) implies both (13a) and (13b), its conservatism is clear. Conditions (13a) and (13b) deal separately with perturbation injected at the system input and output (points 2 and 1, respectively, in Fig. 4); in this case, the system has far more outputs (16) than inputs (7). Clearly, condition (13b) would need to be more conservative in order to cope with a larger number of sources of perturbation.

Conclusions

The results from this study demonstrate how an estimator-based compensator could be designed to be robust with regard to parametric variation and spillover from the dynamics not included in the design model. In particular, the compensator has been shown to be highly robust to variations in the numerical accuracy of the controller gains.

The eighnvalue method, as applied to the MSAT example here, has been shown to be quite effective in arriving at a robust solution. However, the results are still subject to the limitations of the evaluation model assumed. In particular, one cannot draw any conclusion regarding the effects of either parametric variation in the evaluation model or the residual modes excluded from the model in the first place.

The singular value method results in a considerably more conservative design (in the sense of producing a controller with a relatively smaller bandwidth) but has the advantage of providing built-in robustness for a broad class of perturbation dynamics, whether structured or not. Furthermore, the criteria provide a useful stability margin interpretation in terms of bounds on the magnitude of the unmodeled residual dynamics. This has important implications for flexible spacecraft control problems since most of the high-frequency modes as well as the damping factors in the evaluation model are typically not known with certainty.

Both methods, however, can only produce local results in the sense that the outcome depends entirely on the starting values of the "tuning" parameters that have been inserted into the measurement noise intensity and the control input cost weighting function. Much remains to be investigated on the theoretical front before a global design tool for flexible spacecraft is available.

Acknowledgments

This work was supported by the Department of Communications (DOC) of Canada under DSS Contract 06ST.36001-3-2484. The first author would like to thank the Communications Research Centre of DOC for providing Spar with the use of KEDDC, a computer-aided control system design software package, during the tenure of this contract.

References

[1]Davison, E.J. and Gesing, W., "A Study on the Control of Third Generation Spacecraft," *Proceedings of Workshop on Identification and Control of Large Space Structures,* San Diego, CA, 1984.

[2]Stieber, M.E., "Design and Evaluation of Control Systems for Large Communications Satellites," *Proceedings of Workshop on Identification and Control of Large Space Structures,* San Diego, CA, 1984.

[3]Yuan, J.S-C., "Demonstration of Flexible Spacecraft Control Design Software and Techniques—Final Report," DOC-CR-84-020, Dept. of Communications, Canada, May 1984.

[4]Hughes, P.C., "Development of Dynamics Model and Control System Design of Third Generation Spacecraft—Executive Summary," DOC-CR-SP-82-056, Dept. of Communications, Canada, Aug. 1982.

[5]Hughes, P.C. and Skelton, R.E., "Modal Truncation for Flexible Spacecraft," *Journal of Guidance and Control,* Vol. 4, May-June 1981, pp. 291-297.

[6]Kwakernaak, H. and Sivan, R., *Linear Optimal Control Systems,* John Wiley & Sons, Inc., New York, 1972.

[7]Doyle, J.C. and Stein, G., "Multivariable Feedback Design: Concepts for a Classical/Modern Synthesis," *IEEE Transactions on Automatic Control,* Feb. 1981, p. 4-16.

[8]Lehtomaki, N.A., Sandell, N.R. Jr., and Athans, M., "Robustness Results in Linear-Quadratic Gaussian Based Multivariable Control Designs, *IEEE Transactions on Automatic Control,* Feb. 1981, pp. 75-93.

[9]Cruz, J.B. Jr., Freudenberg, J.S., and Looze, D.P., "A Relationship Between Sensitivity and Stability of Multivariable Feedback Systems," *IEEE Transactions on Automatic Control,* Feb. 1981, pp. 66-74.

[10]Kosut, R.L., Salzwedel, H., and Emami-Naeini, A., "Robust Control of Flexible Spacecraft," *Journal of Guidance, Control and Dynamics,* Vol. 6, March-April 1983, pp. 104-111.